Single-Particle Colloid Tracking in Four Dimensions

Stephen M. Anthony,† Liang Hong,‡ Minsu Kim,§ and Steve Granick*,†,‡,§

Departments of Chemistry, Materials Science and Engineering, and Physics, University of Illinois, Urbana, Illinois 61801

Received July 18, 2006. In Final Form: September 22, 2006

Coating a close-packed fluorescent colloid monolayer with a nanometer-thick metal film followed by sonication in liquid produces modulated optical nanoprobes. The metal coating modulates the fluorescence as these structures rotate in suspension, enabling the use of these particles as probes to monitor both rotational and center-of-mass (translational) dynamics in complex environments. Here, we demonstrate methods to simultaneously measure two translational and two rotational degrees of freedom, with excellent agreement to theory. The capability to determine two angles of rotation opens several new avenues of future research.

Introduction

Colloids are widely found both in nature and technology. Particles in this size range (larger than molecules but small enough to sustain Brownian motion) are employed in diverse applications, including paints, ceramics, and photonic materials.[1] Models of crystal growth,[2,3] glass transition,[4,5] and material fracture[6,7] are all studied with colloids serving as convenient proxies for atoms, as they present the great advantage of being visible in an optical microscope. Translational diffusion of colloidal particles has been widely studied. Its study (especially in dense suspensions) comprises a major theme of modern colloid science.[8,9]

Here, we demonstrate a general method to measure concurrently the rotational diffusion of colloidal particles. We validate this method by comparison with theoretical models in the model system to which this method was applied as proof-of-principle, spherically shaped particles at dilute concentrations.

Alternative methods to study the rotational diffusion of colloids are limited. For example, time-resolved fluorescence anisotropy is used widely to study the rotational diffusion of molecules,[10] but it cannot be used to study rotation whose time scale is longer than the fluorescence lifetime of a fluorescent dye, which is on the order of nanoseconds. A further complication involves the distinction between single-particle behavior and its ensemble average. The ensemble-average rotational diffusion of colloids has been studied using dynamic light scattering and fluorescence recovery after photobleaching,[11,12] but these methods cannot track the rotational diffusion of single particles. Thus, they cannot dissect the constituent elements that comprise an ensemble.

Recently, modulated optical nanoprobes (MOONs), an approach introduced by Kopelman and co-workers, showed that rotational diffusion can be tracked with single-particle resolution.[13,14] The idea is that, by coating one hemisphere of fluorescent microspheres with a thin layer of reflective metal, modulation of the excitation and emission of fluorescence occurs when this particle rotates. When viewed and magnified in an appropriate microscope, images of such particles mimic the moon in all its phases (see Figure 1, discussed below). This introduces the possibility of tracking, at the single-particle level, two rotational degrees of freedom simultaneously.[15] Here, we present techniques to rapidly and accurately measure the orientation of two axes of a MOON particle from a single image, thus enabling one to calculate rotational dynamics when successive frames are considered. Another innovation is the capability of locating the center of the MOON particles, regardless of their orientation. Analyzing these positions using standard single-particle tracking techniques,[8,16] enables the simultaneous determination of center-of-mass (translational) diffusion, allowing one to compare translation and rotation, particle by particle.

Experiment and Data Analysis

Samples. MOONs were prepared using monodisperse solutions of 2 μm carboxylate-modified polystyrene latex particles labeled with red fluorescence (F8826 from Invitrogen, Inc., lot 42514A), using standard techniques.[13] One hemisphere of these particles was coated with a 30 nm thick coating of gold, followed by suspension in aqueous solution. The size distribution was less than 2%.

Microscopy Methods. Images were collected using epifluorescence microscopy using a 532 nm laser focused at the rear focal point of the objective. A 63× long working distance objective with 2.5× post-magnification provided good resolution while maintaining sufficient depth of field to image the entire MOON in its trajectory. The fluorescence image was collected using the same objective and recorded by a back-illuminated electron multiplying CCD camera (Andor Ixon) after filtering out light from the excitation laser.

The dynamic data were recorded with an exposure time of 50 ms, with 1500 frames captured. The concentration of particles for all experiments was <1% in an aqueous solution. These concentrations were sufficiently low to avoid multibody interactions.

* Corresponding author.
† Department of Chemistry.
‡ Department of Materials Science and Engineering.
§ Department of Physics.

(1) Qi, M. H.; Lidorikis, E.; Rakich, P. T.; Johnson, S. G.; Joannopoulos, J. D.; Ippen, E. P.; Smith, H. I. *Nature (London)* **2004**, *429*, 538.
(2) Pusey, P. N.; Van Megen, W.; Barlett, P.; Ackerson, B. J.; Rarity, J. G.; Underwood, S. M. *Phys. Rev. Lett.* **1998**, *63*, 2753.
(3) Gasser, U.; Weeks, E. R.; Schofield, A.; Pusey, P. N.; Weitz, D. *Science* **2003**, *292*, 258.
(4) van Blaaderen, A.; Wiltzius, P. *Science* **1995**, *270*, 1177.
(5) Yethiraj, A.; Van Blaaderen, A. *Nature* **2003**, *421*, 513.
(6) van Blaaderen A. *Science* **2003**, *301*, 470.
(7) Schall, P.; Cohen, I.; Weitz, D.; Spaepen, F. *Science* **2004**, *305*, 1948.
(8) Crocker, J. C.; Grier D. G. *J. Colloid Interface Sci.* **1996**, *179*, 298−310.
(9) Weeks, E. R.; Crocker, J. C.; Levitt, A. C.; Schofield, A.; Weitz, D. A. *Science* **2000**, *287*, 627.
(10) Lakowicz, J. R. *Principles of Fluorescence Spectroscopy*, 2nd ed.; Springer: New York, 1999.
(11) Cicerone, M. T.; Blackburn, F. R.; Ediger, M. D. *J. Chem. Phys.* **1995**, *102*, 471.
(12) Kanetaks, J.; Tolle, A.; Sillescu, H. *Phys. Rev. E* **1997**, *55*, 3006.
(13) Anker, J. N.; Kopelman, R. *Appl. Phys. Lett.* **2003**, *82*, 1102.
(14) Anker, J. N.; Behrend, C.; Kopelman, R. *J. Appl. Phys.* **2003**, *93*, 6698.
(15) Behrend, C. J.; Anker, J. N.; McNaughton, B. H.; Braseul, M.; Philbert, M. A.; Kopelman, R. *J. Phys. Chem. B* **2004**, *108*, 10408.
(16) Anthony, S. M.; Zhang, L.; Granick, S. *Langmuir* **2006**, *22*, 5266.

10.1021/la062094h CCC: $33.50
Published on Web 10/19/2006

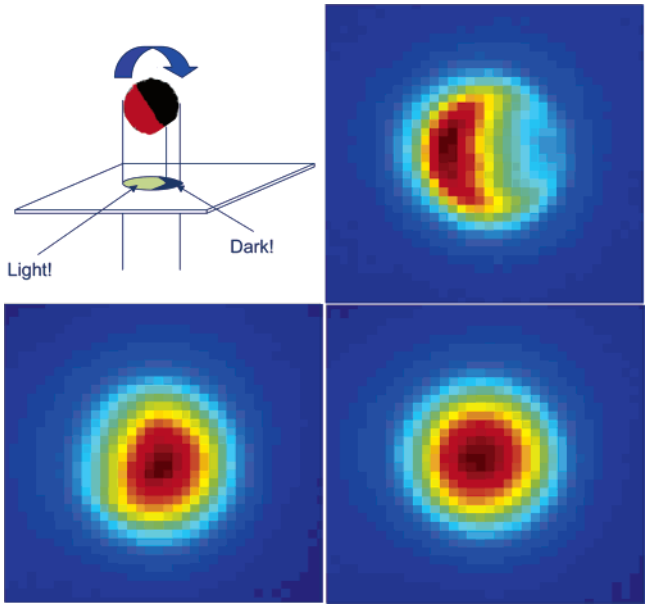

Figure 1. The idea of measuring rotational diffusion using MOON particles, fluorescent on one side and "dark" on the other, is illustrated. (a) Schematic illustration of this idea. (b−d) Images of a MOON particle, 2 μm in diameter, for three orientations ranging from crescent to full moon. The color denotes the varying intensity of the image.

Results and Discussion

Image Analysis. Before any subsequent analysis, first the spatial position of each colloid particle must be located. While many methods are routinely used to locate and track particles, as reviewed by Cheezum et al.,[17] none are appropriate for this problem. For such previously developed techniques, the major concern was signal-to-noise. Here, resolving a particle's fluorescence from the background is not difficult because each particle contains many dyes. But how does one locate the center of a sphere? The problem is that, as a sphere rotates and is visible in MOON fashion, its center is not the center of brightness. (A limiting case is that, when observing the crescent phase, the center of the sphere will display no fluorescence at all.)

However, largely unaffected by the orientation of the MOON particle, the high contrast between its fluorescence and the background allows a different method of locating the spatial position of the particle, provided that the particle is divided into hemispheres (which, for the systems studied here, we confirmed by scanning electron microscopy). The idea is that, regardless of the observed phase of a MOON particle, the bright region should always contain two points separated by the diameter of the MOON. Therefore, if this image is convoluted with a circle having the same diameter of the MOON, the location of the brightest point corresponds to the center of the MOON, since a circle centered at any other point cannot completely contain the bright region. The idea is illustrated in Figure 2 and discussed below.

Having located the position of the MOON, the next challenge is to determine its angular orientation relative to the observer, in the microscope. The convention we chose specified the center of the bright hemisphere of the MOON, with $\theta = 0°$ corresponding to the full moon orientation, and φ corresponding to the orientation within the plane of the image, from the perspective of the experimental observer. Therefore, assuming hemispherical coating, the total brightness of the feature after subtraction of the background is approximately cosinusoidal:

$$A \times (1 + \cos \theta) \tag{1}$$

with corrections for imperfect coating described elsewhere.[18] For this purpose, the depth of focus can be neglected, since the primary effect of being slightly out of focus is to blur the image; thus, as long as the region used to determine the brightness is large enough, the total brightness is unaffected. While eq 1 represents a convenient approximation, the exact formula can be determined by calculating the fraction of the volume of the sphere not obstructed from view by the metal coating:

$$A \times \left(1 - \frac{\theta}{\pi} + \frac{9}{64}\cdot\sin(2 \times \theta)\right) \tag{2}$$

For sufficiently long "movies" of consecutive time series of images, all orientations will be sampled, and the brightest value of the MOON reveals the value of A after background correction. Alternatively, for shorter movies, it is possible to select images with easily determined θ, such as half-moon orientation, and also calculate A.

Independently, we can determine the azimuthal angle, φ, which, to the best of our knowledge, has not been calculated previously in the study of colloidal particle rotation, from a single image. For all orientations other than $\theta = 0°$ or 180° (in which case φ is irrelevant), both light and dark portions of the MOON are observed. The azimuthal angle φ of the MOON can be determined from the orientation of the line connecting the center of the MOON, located previously, with the center of the bright pixels

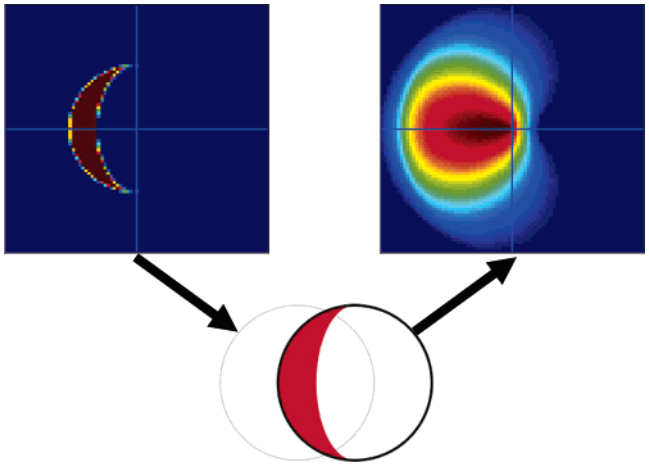

Figure 2. How to locate the center of mass of MOON particles, whose fluorescence image is inherently anisotropic depending on how the particle is oriented relative to the observer. Left top panel: simulated image produced by a MOON in the crescent phase, its center located at the indicated cross-hairs. Note that, regardless of orientation relative to the observer, the bright region will always have two points separated by the diameter of the MOON. Note also that diffraction blurs the experimental images, but that, for clarity, diffraction-blurring was not calculated for the simulated images. Bottom panel: one sole circle whose diameter matches the MOON's diameter contains the fluorescent image completely. Top right panel: Image produced by convoluting the original image with a circle of this same diameter. The maximum in this image corresponds to the deduced center of the MOON. Uncertainty in its location is greater parallel to the tilt of the MOON than perpendicular to it; however, error in this direction has no effect upon calculating the azimuthal angle. The color at each point indicates the relative quality of the overlap between a circle centered at this point and the crescent at left, with the best overlap corresponding to the centered circle.

(17) Cheezum, M. K.; Walker, W. F.; Guilford, W. H. *Biophys. J.* **2001**, *81*, 2378.

(18) Hong, L.; Anthony, S. M.; Granick, S. *Langmuir* **2006**, *22*, 7128.

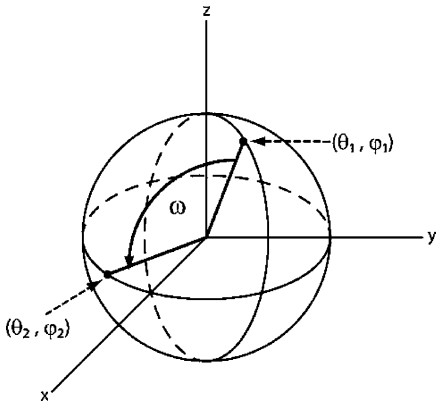

Figure 3. The measured quantities, θ and φ, completely specify the position of the bright hemisphere of the MOON at any given time. When determining rotational diffusion, we are less interested in the specific orientation of the MOON than in how far the MOON has rotated from its previous position. Therefore, the angle of variation, ω, is computed over the given time interval.

of the image, mathematically specified by the centroid of that portion of the image. Most uncertainty in locating the center of the MOON is collinear with this line, and thus this error does not propagate into calculating the angle. In principle, the zenith angle, θ, can also be determined from the distance separating the two points that define the line. However, for typical image sizes, this method is less accurate than the one just described, especially since here the error in locating the center of the MOON becomes relevant.

The combination of θ and φ completely specifies the orientation of one axis of the sphere. As time goes by, the orientation of this axis changes. The rotation of this axis with time is specified by the angle of variation, ω, as shown in Figure 3. Using this quantity, we can determine the rotational diffusion constant, D_r, using formulas developed long ago by Perrin.[19] For small angular displacements, the approximation

$$\langle \omega^2 \rangle = 4D_r\Delta t \tag{3}$$

can be employed; however, the rigorous formula incorporating the effects of the bounded nature of angles is

$$\langle \sin^2 \omega \rangle = \frac{2}{3}(1 - e^{-6D_r\Delta t}) \tag{4}$$

which can be rewritten as

$$-\ln\left(1 - \frac{3}{2}\langle \sin^2 \omega \rangle\right)/6 = D_r\Delta t \tag{5}$$

In both cases, the uncertainty in ω can be determined from the intercept at $\Delta t = 0$. Using these formulas, it becomes possible to more accurately determine the rotational diffusion with a shorter time window.

Data Analysis. Following standard procedures for particle tracking, when computing the mean squared displacement for time step t, each trajectory is subdivided into as many segments of length t as possible with no overlap, and averaging is conducted over all these segments from all the particles. Similar averaging was employed when computing the rotational diffusion. Slopes were determined using weighted least-squares linear regression.

When working with data concerning center-of-mass displacement, the confidence intervals for each point were determined based upon the number of segments averaged to form that point,

(19) Perrin, F. *Ann. Sci. Ecole Normale Super.* **1928**, *45*, 1.

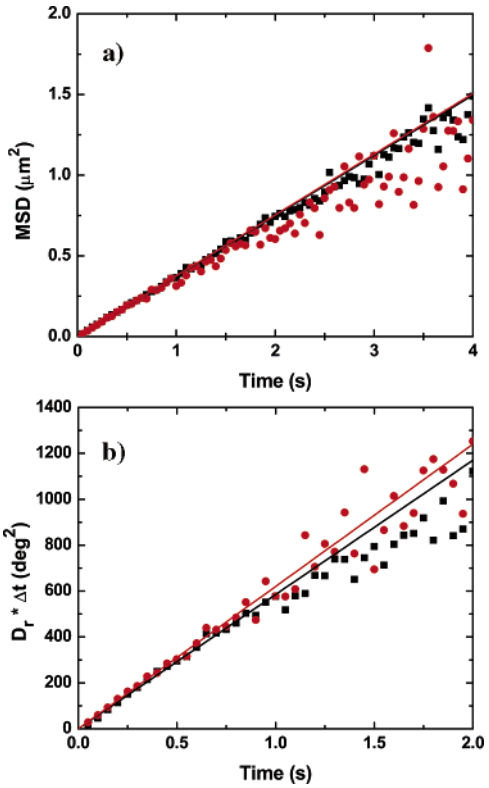

Figure 4. The efficacy to quantify the rotational and translational diffusion of colloidal-sized MOON particles is illustrated. (a) The translational data are plotted both for the average of six particles (black squares) and for a single MOON particle (red circles). As described in the text, fitting yielded an ensemble-average translational diffusion constant for the 2 μm MOONs of 0.094 $\pm$ 0.003 μm^2/s (black line). Based on the y-intercept of 0.0033 μm^2, the uncertainty in position for the MOONs is 0.04 μm. As can be seen from the virtual overlap of the two fits, while the ensemble data is obviously less noisy, information from a single trajectory of a single particle can be analyzed quantitatively with the same conclusion. (b) As a result of the boundary conditions on angular displacements, the mean squared angular displacement is an approximation limited in utility to small angles. Here, the more rigorous formula (eq 5), which accounts for these limitations, is employed. (The left side of eq 5, equivalent to $D_r \times \Delta t$, is plotted here.) The resulting ensemble-average rotational data for the 2 μm MOONs (black squares) is nicely linear. A vertical offset of 82 deg^2, resulting from the angular uncertainty of 14°, was subtracted. The slope of this plot yields a rotational diffusion coefficient of 585 $\pm$ 35 deg^2/s (black line). For comparison, similar data for a single MOON is also shown (red circles). From even this single MOON particle, it is possible to determine the rotational diffusion constant of 620 $\pm$ 100 deg^2/s, albeit with lower accuracy (red line). The deviations from the linear fits after around 1 s are not significant, as the uncertainty of those points is much greater. Additionally, the error for those points is not normally distributed, such that, on average, one should expect to observe a downward curvature.

and were highly asymmetric when the sample size was small. However, when the sample size was large enough to allow averaging over more than 100 segments, the uncertainty for each point was found to be approximately normally distributed (skewness and residual kurtosis < 1).

Because weighted linear regression assumes that uncertainty is normally distributed, only data that satisfied this criteria were used in subsequent calculations of the diffusion coefficient. Note that the fitting uncertainty was negligible compared to systematic uncertainties such as polydispersity (see below).

Application to a Specific System. We selected a spherical colloid particle at dilute concentrations because, for this case,

the theoretical predictions are clear-cut and the comparison of this new experiment to theory would be most unequivocal.

Analysis of the time sequence of images confirmed the ability to monitor translation of this particle and its rotation concurrently, as well as the ability to distinguish between MOON particles and other particles. The findings described below are based on six particle trajectories in elapsed time, each lasting 75 s. The observation period for the retained trajectories was sufficient to observe them rotate completely, allowing the zenith angle to be determined from the brightest and dimmest points. In Figure 4b, the rotational dynamics are plotted according to eq 5. From the slope of the linear fit, the rotational diffusion constant was found to be 0.178 rad^2/s, that is, 585 ± 35 deg^2/s. Since the reported error was based upon the variation in the computed rotational diffusion constant throughout the time sequence, this error represents the error in measurement for this sample, but does not include the error introduced by the polydispersity, This agrees well with the Debye−Stokes−Einstein rotational diffusion constant of 540 deg^2/s for a 2 μm sphere.

Upon the basis of the *y*-intercept, our average uncertainty in orientation was 14°. This would suggest an average uncertainty of approximately 10° in our determination of the zenith and azimuthal angles. However, it is important to note that the uncertainty in these measurements itself depends on the zenith angle. With respect to the zenith angle, accuracy decreases when the zenith angle is near one of its extreme bounds. Since there exists an approximately cosinusoidal relationship between the zenith angle and the brightness, smaller uncertainties in brightness produce correspondingly larger uncertainties in the zenith angle when it is near its extreme values. Similarly, determining the angle of the azimuth depends on the zenith angle. For a zenith angle of 90° (half moon), the azimuthal orientation is clear; however, as the zenith approaches its limits, discerning the azimuthal orientation becomes increasingly difficult.

Simultaneously, the translational dynamics were determined (Figure 4a). Contributing to the faithfulness of particle tracking in this respect is our ability to track the center-of-mass of the particle, which must be distinguished from its center of brightness. From the *y*-intercept of 0.0033 μm^2, the uncertainty in position for the MOONs is 0.04 μm, or approximately 1/2 pixel, which is not surprising since the image-analysis algorithms we use[18] locate positions to the nearest pixel in the interest of computational efficiency. Upon the basis of the slope, the translational diffusion constant was determined to be 0.094 ± 0.003 μm^2/s.

This is less than would be anticipated from the Stokes−Einstein equation for dilute particles of this diameter in solution (0.22 μm^2/s), but reflection shows this finding to be unsurprising when the hydrodynamic influence of the nearby wall is considered. Recall that the particle whose time-dependent position we tracked had previously sedimented to near the bottom of the sample cell. The expected ratio of diffusion parallel to this "wall", relative to bulk diffusion, is given by

$$\frac{D}{D_0} = 1 - \frac{9}{16}\frac{r}{z} + 18\left(\frac{r}{z}\right)^3 - \frac{45}{256}\left(\frac{r}{z}\right)^4 - \frac{1}{16}\left(\frac{r}{z}\right)^5 \qquad (6)$$

where r is the radius of the particle and z is the separation of the center of the particle from the wall.[20] Assuming a Boltzmann distribution based upon gravitational potential energy for the separation of the particles from the wall and given the calculated density of the MOON particles, 1.45 g cm^{-3}, the mean distance between the bottom of the particle and the wall is 0.22 μm. Then, considering the Boltzmann distribution of in-plane diffusion coefficients of particles located at each expected distance from the wall, the expected ratio of these quantities is 0.47, which should be compared with the observed ratio of 0.45. This is excellent agreement, especially considering that this estimate does not even consider the second-order effect that particles also diffuse normal to the solid surface.

This simple method to determine the orientation of MOON particles shows how to determine the position of the center of the bright hemisphere uniquely specified within each image, according to each individual particle whose Brownian motion is tracked. Of paramount importance is to simultaneously observe two of the rotational and two of the translational degrees of freedom.

These experimental approaches are not important in their own right; they just confirm known theories for the simple model system that we studied intentionally to validate the technique. The main point is that they point the way toward applying these methods of single-particle tracking in new directions, the most prominent among them being to study the translational−rotational coupling of colloids in concentrated suspensions.[21−25] Apart from an intriguing light scattering study by Bonn and co-workers of colloidal disks,[26] we note that the vast literature on translation−rotation coupling regarding molecules is not yet accompanied by data concerning colloids.

Acknowledgment. S.A. acknowledges the NSF for financial support in the form of a Graduate Research Fellowship. This work was supported by the donors of the Petroleum Research Fund, administered by the American Chemical Society (ACS). We also acknowledge use of facilities purchased with grants NSF-DMR-0605947 and NSF-CMS-0555820.

LA062094H

(20) Faucheux, L. P.; Libchaber, A. J. *Phys. Rev. E.* **1994**, *49*, 5158.
(21) Pham, K. N.; Puertas, A. M.; Bergenholtz, J.; Egelhaaf, S. U.; Moussaid, A.; Pusey, P. N.; Schofield, A. B.; Cates, M. E.; Fuchs, M.; Poon, W. C. K. *Science* **2002**, *296*, 104.
(22) Gebremichael, Y.; Vogel, M.; Bergroth, M. N. J.; Starr, F. W.; Glotzer, S. C. *J. Phys. Chem. B* **2005**, *109*, 15068.
(23) Qiu, X. H.; Ediger, M. D. *J. Phys. Chem. B* **2003**, *107*, 459.
(24) Veniaminov, A.; Sillescu, H.; Bartsch, E. *J. Chem. Phys.* **2005**, *122*, 174902.
(25) Kegel, W. K.; van Blaaderen, A. *Science* **2000**, *287*, 290.
(26) Jabbari-Farouji, S.; Eiser, E.; Wegdam, G. H.; Bonn, D. *J. Phys.: Condens. Matter* **2004**, *16*, L471.